Neuron, Volume *75*

Supplemental Information

Metabolic Communication between Astrocytes and Neurons via Bicarbonate-Responsive Soluble Adenylyl Cyclase

Hyun B. Choi, Grant R.J. Gordon, Ning Zhou, Chao Tai, Ravi L. Rungta, Jennifer Martinez, Teresa A. Milner, Jae K. Ryu, James G. McLarnon, Martin Tresguerres, Lonny R. Levin, Jochen Buck, and Brian A. MacVicar

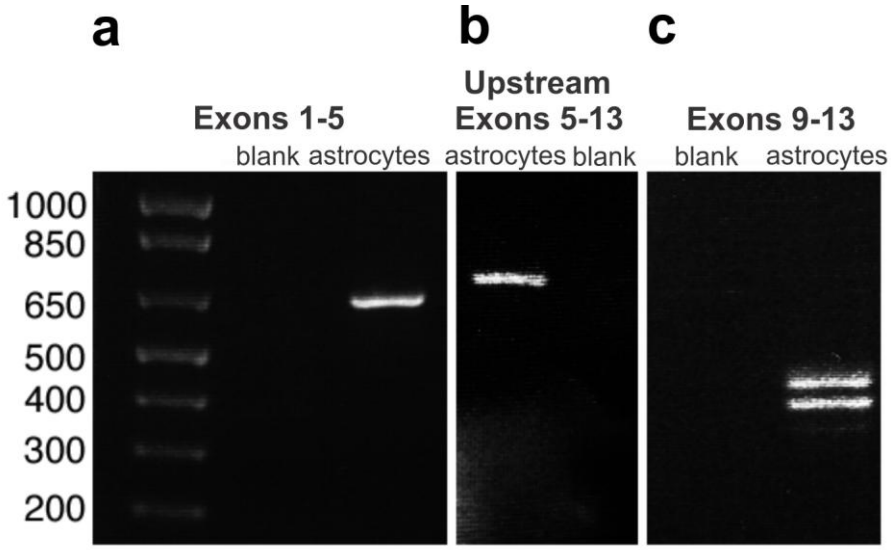

Figure S1. Rat astrocytes possess mRNAs coding for various soluble adenylyl cyclase splice variants. RT-PCR detected transcripts corresponding to (a) sAC (exons 1-5) (b) sACsomatic which starts at the alternate promoter upstream from exon 5 and (c) sACt (lower band lacks exon 12, resulting in an early stop codon) and sACfl (higher band).

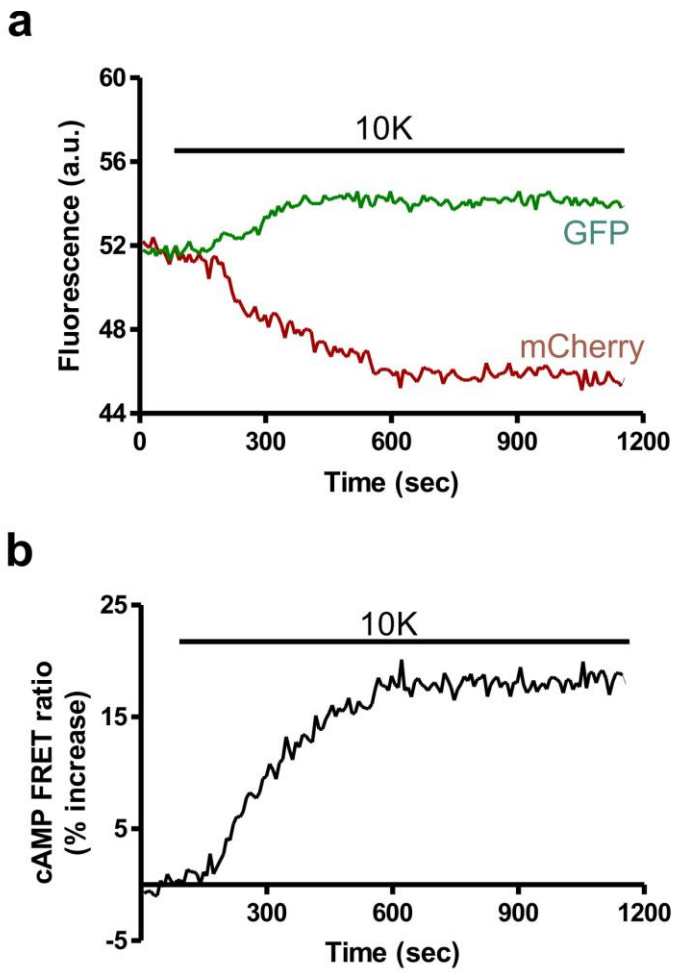

Figure S2. Representative GFP and mCherry fluorescence emissions from a single astrocyte transfected with gene encoding GFPnd-EPAC(dDEP)-mCherry cAMP FRET sensor. (a) Application of high $[K^+]_{ext}$ (10 mM) induced a significant increase in GFP fluorescence (green trace), and decrease in mCherry fluorescence (red trace) respectively. (b) 10 mM $[K^+]_{ext}$ induced an increase of the cAMP FRET ratio (GFP/mCherry).

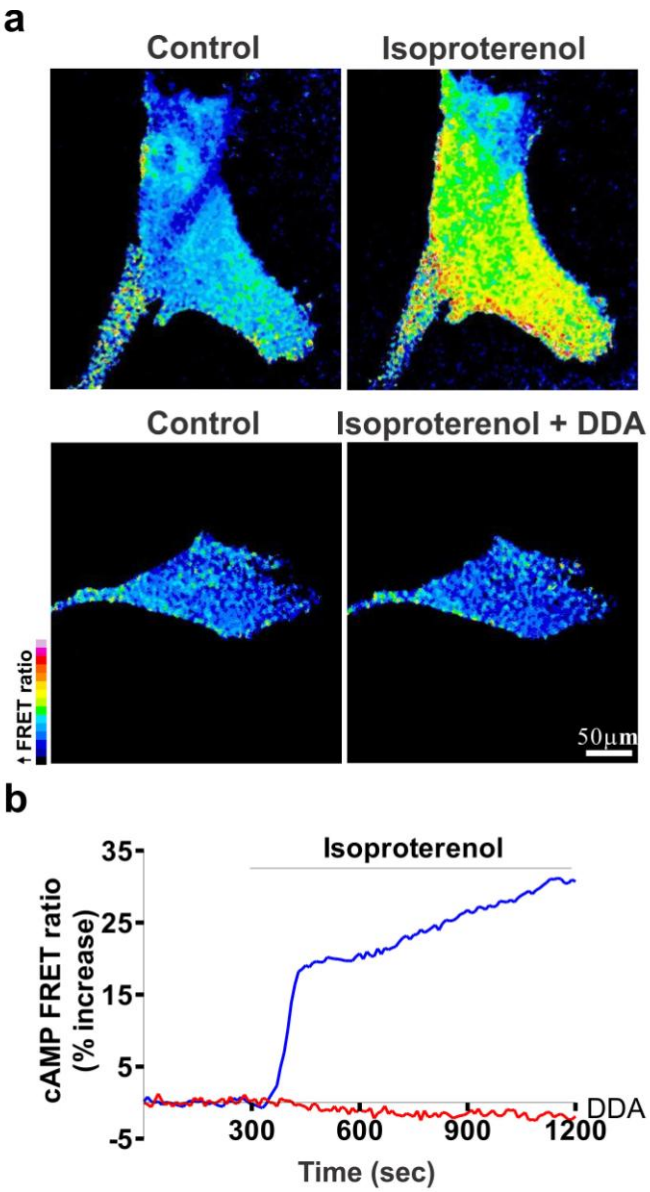

Figure S3. Activation of beta-adrenoreceptor increases cAMP FRET ratio in cultured astrocytes. (a) Representative FRET images before and after treating with isoproterenol (100 μM). Isoproterenol induced a significant increase of cAMP FRET ratio which was blocked by the tmAC inhibitor, DDA (50 μM). (b) The traces of cAMP FRET ratio (GFP/mCherry) induced by isoproterenol alone (blue trace) and together with DDA (red trace).

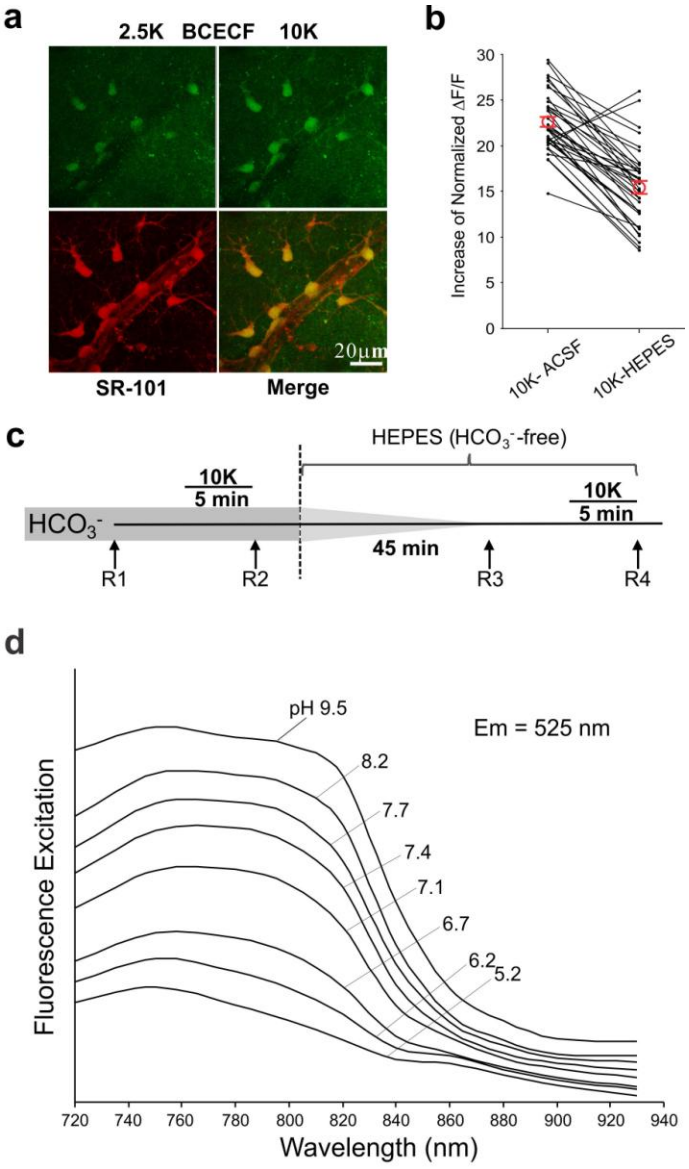

Figure S4. High K^+ induces an intracellular alkaline shift. (a-b) Two-photon images showing that high K^+ induces widespread alkalinization, indicated by increased BCECF fluorescence, in astrocytes identified by SR-101 staining. The alkalinization was reduced in HCO_3^--free solution (replaced with HEPES buffered aCSF). (c) A timeline of the experiment for measuring intracellular pH using BCECF. Region 1 (R1) and R3 represent control recording in the presence and absence of bicarbonate, respectively. R2 and R4 correspond to recording with high K+ in the presence and absence of bicarbonate, respectively. (d) Two-photon excitation spectrum of BCECF at different extracellular pH normalized for power at different wavelengths.

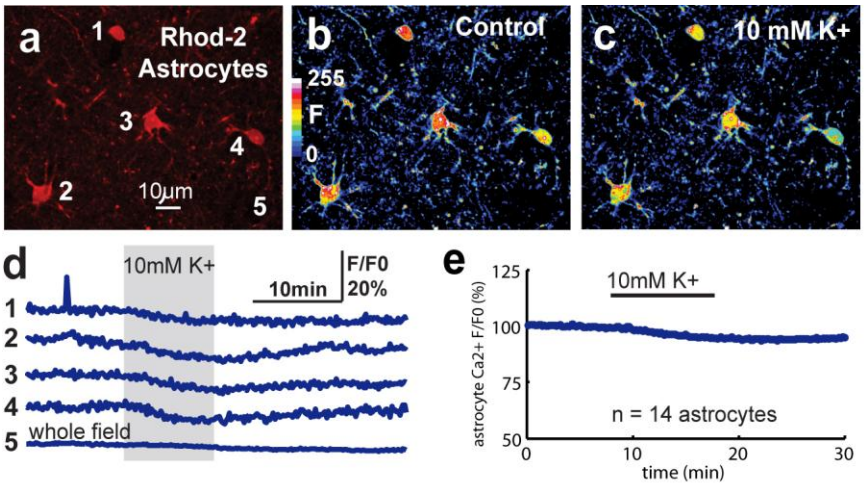

Figure S5. High $[K^+]_{ext}$ does not induce changes of intracellular free $[Ca^{2+}]$ in astrocytes. (a) Astrocytes loaded with a calcium indicator dye, Rhod-2/AM. (b-c) Intracellular free $[Ca^{2+}]$ changes before (b) and after (c) high $[K^+]_{ext}$ (10 mM) application. (d) Individual traces of intracellular free $[Ca^{2+}]$ changes in 4 astrocytes labelled in (a) and whole field labelled as 5. (e) Pooled data from 14 astrocytes.

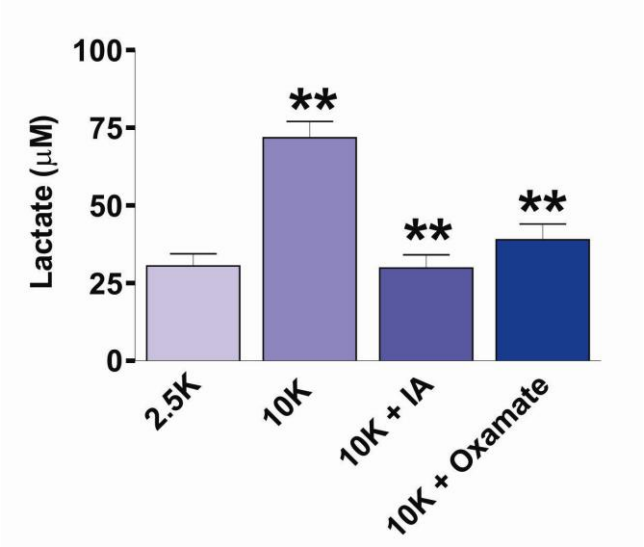

Figure S6. High $[K^+]_{ext}$-mediated lactate production was significantly reduced in the presence of iodoacetate (IA, 200 μM), an inhibitor of GAPDH, and oxamate (2.5 mM), an inhibitor of LDH. Error bars indicated SEM.

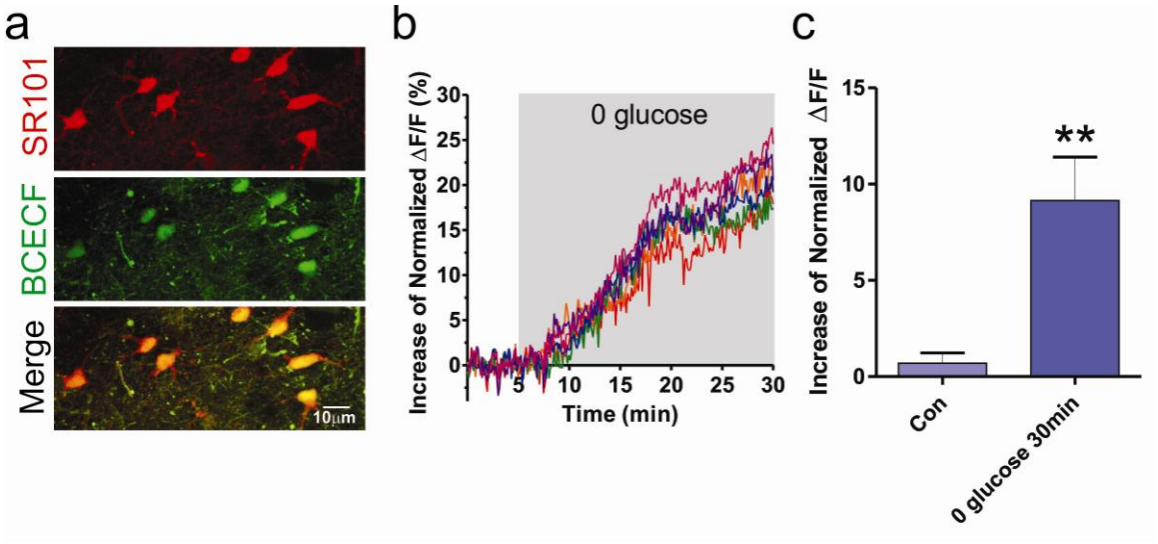

Figure S7. Aglycemia induces an intracellular alkaline shift. (a) Two-photon images showing BCECF fluorescence, in astrocytes identified by SR-101 staining. (b) Typical traces showing an increase of BCECF fluorescence when glucose is removed from aCSF. (c) Pooled data showing an alkalinization of astrocytes in an aglycemic condition. Error bars indicate SEM.